

# Probability of a zoonotic spillover with seasonal variation

Aadrita Nandi <sup>a, b</sup>, Linda J.S. Allen <sup>a, \*</sup>

<sup>a</sup> Department of Mathematics and Statistics, Texas Tech University, Lubbock, TX, 79409-1042, USA

<sup>b</sup> Department of Microbiology and Immunology, University of Michigan Medical School, Ann Arbor, MI, 48108-5260, USA



## ARTICLE INFO

### Article history:

Received 19 November 2020

Received in revised form 19 January 2021

Accepted 19 January 2021

Available online 4 March 2021

Handling Editor: Dr. J Wu

### 2010 MSC:

60J27

60J85

92D30

### Keywords:

Branching process

Markov chain

Seasonal fluctuations

Spillover

Zoonoses

## ABSTRACT

Zoonotic infectious diseases are spread from animals to humans. It is estimated that over 60% of human infectious diseases are zoonotic and 75% of them are emerging zoonoses. The majority of emerging zoonotic infectious diseases are caused by viruses including avian influenza, rabies, Ebola, coronaviruses and hantaviruses. Spillover of infection from animals to humans depends on a complex transmission pathway, which is influenced by epidemiological and environmental processes. In this investigation, the focus is on direct transmission between animals and humans and the effects of seasonal variations on the transmission and recovery rates. Fluctuations in transmission and recovery, besides being influenced by physiological processes and behaviors of pathogen and host, are driven by seasonal variations in temperature, humidity or rainfall. A new time-nonhomogeneous stochastic process is formulated for infectious disease spread from animals to humans when transmission and recovery rates are time-periodic. A branching process approximation is applied near the disease-free state to predict the probability of the first spillover event from animals to humans. This probability is a periodic function of the time when infection is introduced into the animal population. It is shown that the highest risk of a spillover depends on a combination of animal to human transmission, animal to animal transmission and animal recovery. The results are applied to a stochastic model for avian influenza with spillover from domestic poultry to humans.

© 2021 The Authors. Publishing services by Elsevier B.V. on behalf of KeAi Communications Co. Ltd. This is an open access article under the CC BY-NC-ND license (<http://creativecommons.org/licenses/by-nc-nd/4.0/>).

## 1. Introduction

Zoonotic infectious diseases, transmitted from wild or domestic animal hosts to humans, result in over 60% of human infectious diseases with 75% of them emerging diseases (Guo et al., 2020; Jones et al., 2008; Karesh et al., 2012; Taylor et al., 2001; WHO, 2020b). Many emerging zoonotic diseases are caused by viruses such as avian influenza virus, Ebola virus, rabies virus, severe acute respiratory syndrome coronavirus-1 (SARS-CoV-1), SARS-CoV-2, Middle East respiratory syndrome coronavirus (MERS-CoV), West Nile virus, Nipah virus, Hendra virus and hantaviruses (Han et al., 2015; Poen et al., 2019). A zoonotic spillover occurs when the pathogen from an infected animal host enters a human host, either directly from a natural reservoir, an intermediate animal host, or indirectly from virus in the environment. For example, avian influenza often spills over to humans from an intermediate host (domestic poultry) instead of directly from the natural reservoir (waterfowl

\* Corresponding author.

E-mail address: [linda.j.allen@ttu.edu](mailto:linda.j.allen@ttu.edu) (L.J.S. Allen).

Peer review under responsibility of KeAi Communications Co., Ltd.

including ducks and geese) (Poen et al., 2019; Vandegrift et al., 2010). For hantaviruses, spillover into humans generally occurs via contact with infected excreta from the natural reservoir, such as rats, mice or voles (Jonsson et al., 2010).

Spillovers of public health concern are those involving new pathogens that enter the human population. Animal reservoirs vary considerably, but bats and rodents are the majority of natural reservoirs for viral zoonoses originating in the wild (Calisher et al., 2006; Han et al., 2015; Luis et al., 2013). The natural reservoirs for rabies virus, coronaviruses, Ebola virus, Nipah virus and Hendra virus are bats (Calisher et al., 2006; Cui, Eden, Holmes, & Wang, 2013; Guo et al., 2020; Han et al., 2015; Lau et al., 2005). The Centers for Disease Control and Prevention (CDC), U.S. Department of the Interior and U.S. Department of Agriculture prepared a list of eight zoonotic diseases of most concern to the United States. These eight zoonoses include zoonotic influenza, salmonellosis, West Nile fever, plague, emerging coronavirus diseases, rabies, brucellosis and Lyme disease (CDC, 2019a). Four of the eight pathogens are viruses.

Zoonotic diseases can be transmitted to humans directly or indirectly. Direct or indirect transmission requires contact between the animal source and humans or contact with the pathogen in the environment. These contacts are often driven by environmental factors, especially seasonal variations in temperature, humidity and rainfall that impact food resources and habitat e.g., (Glass et al., 2000; Karesh et al., 2012; Martinez, 2018; Plowright et al., 2017).

With the exception of vector-host epidemic models, much of the modeling efforts for emerging viral zoonoses have concentrated on the disease dynamics within a single population, either humans or the natural reservoir. There are a number of zoonotic modeling studies that include at least two species, such as models for avian influenza (Gumel, 2009; Iwami et al., 2007; Liu et al., 2017; Royce and Fu, 2020; Tuncer & Martcheva, 2013; Vaidya & Wahl, 2015; Zhang et al., 2019), rabies (Asamoah, Oduro, Bonyah, & Seidu, 2017; Huang et al., 2019; Ruan, 2017), hantaviruses (Allen et al., 2009; Sauvage et al., 2007) and COVID-19 (Chen et al., 2020). Most of these models are systems of ordinary differential equations (ODEs). A few stochastic zoonotic disease models include human spillover or seasonal variability, e.g., (Breban, Drake, Stallknecht, & Rohani, 2009; Keeling & Gilligan, 2000; Singh et al., 2014; Vaidya & Wahl, 2015; Voinson et al., 2018). Breban et al. (2009) and Vaidya and Wahl (2015) included seasonal variability in models for avian influenza in migratory waterfowl, as they move between breeding and wintering sites. Keeling and Gilligan (2000) modeled spillover of bubonic plague for a metapopulation of rats, fleas and humans that included seasonal forcing in the flea carrying capacity. Stochastic simulations of the metapopulation model showed sporadic human outbreaks from subpopulations of endemic rat reservoirs. General stochastic models for spillover to humans from an animal reservoir were studied by Voinson et al. (2018) and Singh et al. (2014). These investigations applied Markov chain and branching process theory to susceptible-infected-recovered (SIR) models to study the number and size of outbreaks. Singh et al. (2014) also investigated the dynamics during the early epidemic stages through estimation of the probability of and time to first human spillover. We apply similar techniques, as in Singh et al. (2014) and Voinson et al. (2018), to investigate the early epidemic dynamics. In addition, we extend their models by including seasonal variability in the parameters and by considering more complex settings.

In this investigation, we develop mathematical methods for study of the first spillover event to humans via direct transmission either from a natural reservoir or an intermediate host. We focus on viral zoonoses. However, the methods can be extended to other zoonotic pathogens and to indirect exposure. The following section describes the underlying SIR ODEs from which the transition rates for the time-nonhomogeneous Markov chain are defined. The branching process approximation is described in Section 3. Then, in Section 4, these new mathematical methods are applied. Numerical examples illustrate how the periodic parameters affect the probability of and time to spillover as a function of the time when infection is introduced into the animal population. In Section 5, the methods are applied to several avian influenza models with spillover from domestic poultry to humans (Tuncer & Martcheva, 2013), where the SIR framework is also generalized to include a latent stage. In the last section, the results are summarized and the public health implications are discussed.

## 2. Spillover model

A system of SIR ODEs serves as a framework for formulation of a stochastic model for spillover. Since we are considering the first spillover event, the human disease dynamics after the spillover are not modeled. Whether an outbreak occurs in the human population depends on human-to-human transmission, human recovery rate (Singh et al., 2014; Voinson et al., 2018) and seasonal effects (Nipa & Allen, 2020).

### 2.1. Deterministic spillover model

A compartmental diagram of the deterministic spillover model is given in Fig. 1. The animal population includes susceptible, infectious and recovered animals, denoted as  $S_a$ ,  $I_a$  and  $R_a$ , respectively. Similarly,  $S_h$ ,  $I_h$  and  $R_h$  denote susceptible, infectious and recovered humans, respectively. The parameter  $\beta_{aa}(t)$  is the transmission rate from animal to animal,  $\gamma(t)$  is the recovery rate of an infected animal and  $\beta_{ah}(t)$  is the transmission rate of animal to human. Each of these rates are time-periodic with a common period  $T$ . The population sizes are constant,  $N_a = S_a + I_a + R_a$  and  $N_h = S_h + I_h + R_h$ . For the human population, we do not consider the recovered state, because our interest is in the first spillover event in the human population. The ODE model for the animal and the human populations is described by the following system:

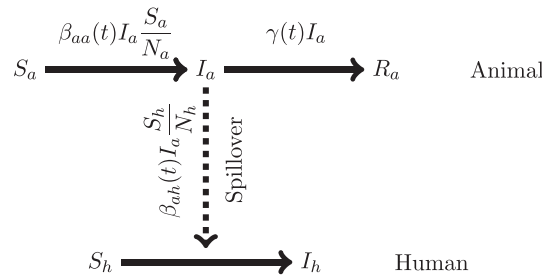


Fig. 1. Compartmental diagram of the SIR ODE model for a spillover event from an animal host (subscript  $a$ ) to a human host (subscript  $h$ ).

$$\text{Animal} \begin{cases} \frac{dS_a}{dt} = -\beta_{aa}(t) \frac{S_a I_a}{N_a} \\ \frac{dI_a}{dt} = \beta_{aa}(t) \frac{S_a I_a}{N_a} - \gamma(t) I_a, \\ \frac{dR_a}{dt} = \gamma(t) I_a, \end{cases} \tag{1}$$

$$\text{Human} \begin{cases} \frac{dS_h}{dt} = -\beta_{ah}(t) \frac{S_h I_a}{N_h}, \\ \frac{dI_h}{dt} = \beta_{ah}(t) \frac{S_h I_a}{N_h}. \end{cases} \tag{2}$$

We assume the parameters are continuous and periodic for  $t \in (-\infty, \infty)$  with common period  $T > 0$ :

$$\gamma(t+T) = \gamma(t), \quad \beta_i(t+T) = \beta_i(t), \quad i = aa, ah. \tag{3}$$

one or more of the rates may be constant or have a fundamental period other than  $T$ .

### 2.2. Stochastic spillover model

The susceptible, infectious and recovered animal and human variables are discrete random variables satisfying

$$S_a(t), I_a(t), R_a(t) \in \{0, 1, \dots, N_a\}, \quad S_h(t), I_h(t), R_h(t) \in \{0, 1, \dots, N_h\}, \quad t \in [0, \infty).$$

the values of the random variables are denoted with lower case letters:  $s_a, i_a, r_a, s_h$  and  $i_h$ . The initial conditions are at a fixed time  $t_0 \in [0, T]$ . They are  $I_a(t_0) > 0$  and  $R_a(t_0) = I_h(t_0) = R_h(t_0) = 0$  with  $S_a(t_0) = N_a - I_a(t_0)$  and  $S_h(t_0) = N_h$ . To record the first spillover event, the stochastic process continues until a time  $t$  ( $t > t_0$ ) such that either  $I_a(t) = 0$  or  $I_h(t) = 1$ . We compute the probability that  $I_h(t) = 1$  before  $I_a(t) = 0$ .

The transition probabilities that lead up to a spillover are described in Table 1. Given  $I_a(t_0) > 0$  and  $I_h(t_0) = 0$ , three possible events may occur: (i) an infected animal infects another animal, (ii) an infected animal recovers or (iii) an infected animal infects a human. Event (iii) is a spillover. The sum of the transition rates is

$$\Sigma(t) = \beta_{aa}(t) i_a \frac{S_a}{N_a} + \gamma(t) i_a + \beta_{ah}(t) i_a \frac{S_h}{N_h}. \tag{4}$$

**Table 1**  
Transition probabilities for a zoonotic spillover,  $r_i(t)\Delta t + o(\Delta t)$ .

Description	Event	$(\Delta I_a, \Delta I_h)$	Probabilities
Animal infection	$(S_a, I_a) \rightarrow (S_a - 1, I_a + 1)$	$(1, 0)$	$\beta_{aa}(t) i_a \frac{S_a}{N_a} \Delta t + o(\Delta t)$
Animal recovery	$(I_a, R_a) \rightarrow (I_a - 1, R_a + 1)$	$(-1, 0)$	$\gamma(t) i_a \Delta t + o(\Delta t)$
Human infection	$(S_h, I_h) \rightarrow (S_h - 1, I_h + 1)$	$(0, 1)$	$\beta_{ah}(t) i_a \frac{S_h}{N_h} \Delta t + o(\Delta t)$
No change	$(S_a, I_a, S_h, I_h) \rightarrow (S_a, I_a, S_h, I_h)$	$(0, 0)$	$1 - \Sigma(t)\Delta t + o(\Delta t)$

To numerically approximate the Markov time-nonhomogeneous process, we use a Monte Carlo approximation based on Table 1. We consider a discrete set of time points  $\{t_n\}_{n=0}^\infty$  with  $t_n = n\Delta t$  for sufficiently small time step  $\Delta t$  so that the probabilities  $r_i(t_n)\Delta t$ ,  $i = 1, 2, 3$  and  $1 - \sum(t_n)\Delta t$  lie in  $[0, 1]$  for  $t_n > 0$ . A uniform random number is used to select the event, if any, that occurs at time  $t_{n+1}$ . An alternate method based on a Gillespie-type algorithm is discussed in Appendix A.

In Fig. 2, five sample paths of the infected animal population are graphed for two different initial conditions. The two initial conditions are  $I_a(t_0) = 1$  for  $t_0 = 0, 1 \in [0, T]$ , where the period length is  $T = 4$ . The sample paths are graphed until the time  $t$ , when either  $I_a(t) = 0$  or  $I_h(t) = 1$ ,  $t > t_0$ , whichever event occurs first. As can be seen in Fig. 2, there are significant differences in the occurrence of a spillover. At  $t_0 = 0$ , transmission rates  $\beta_{aa}(0)$  and  $\beta_{ah}(0)$  and recovery time  $1/\gamma(0)$  are at their peak values; four out of five sample paths result in a spillover. At  $t_0 = 1$ , the values of  $\beta_{aa}(1)$ ,  $\beta_{ah}(1)$  and  $1/\gamma(1)$  have much smaller values than at  $t_0 = 0$  and only one of the five sample paths results in a spillover.

### 3. Branching process approximation

We apply a Markov branching process approximation to the infected animal population, variable  $I_a$ , at the disease-free equilibrium (DFE),  $S_a = N_a$  and  $S_h = N_h$ . In particular, we assume  $I_a$  follows a birth-death-killing process, as defined by Karlin and Tavaré (1982), with state space  $\{0, 1, \dots\} \cup \{K\}$ , where state  $K$  is the first human spillover event. The two states,  $I_a = 0$  and  $I_a = K$  ( $I_h = 1$ ), are the only absorbing states for  $I_a$ . The process begins at a fixed time  $t_0$  and the process stops at time  $t > t_0$ , if either  $I_a(t) = 0$  or  $I_h(t) = 1$ . Karlin and Tavaré (1982) assumed the birth-death-killing process was time-homogeneous with constant parameters. The time-homogeneous process has been applied by Singh et al. (2014) to spillover events for SIR epidemic processes in humans and animals. We extend their work to a time-nonhomogeneous process for periodic transmission and recovery rates and to more general epidemic settings. We summarize some of the theory and describe how the probability of spillover is computed.

The assumptions in the Markov branching process for  $I_a$  are that the population size is unbounded,  $I_a \in \{0, 1, 2, \dots\}$ , the infected animals at time  $t$  are independent of those infected prior to time  $t$  (Markov property) and infected animals produced after a time  $t$  from infected animals at time  $t$  are independent of each other (Harris, 1963). To ensure the branching process is a good approximation of the time-nonhomogeneous process at the human-animal interface, the value of  $N_a$  must be sufficiently large and the initial number of infected animals must be sufficiently small so that the process is near the DFE.

For the Markov branching process, the events in Table 1 simplify to those given in Table 2. Given  $I_a(t_0) = i$ , the branching process is used to estimate the probability of animal disease extinction before the first human spillover. We denote this probability as  $\mathbb{P}_{ext}(i, t_0)$ . The probability of the first human spillover event is  $\mathbb{P}_{spill}(i, t_0) = 1 - \mathbb{P}_{ext}(i, t_0)$ . The derivation of this expression is described below.

The expression for the probability of the first human spillover comes from the more general multitype branching process at the human-animal interface (Singh et al., 2014). The generating function for the interface involves both  $I_a$  and  $I_h$ . Given the transition probability,

$$p_{(i,j),(k,l)}(t_0, t) = \mathbb{P}((I_a(t), I_h(t)) = (k, l) | (I_a(t_0), I_h(t_0)) = (i, j)), \tag{5}$$

the probability generating function for  $(I_a, I_h)$  equals

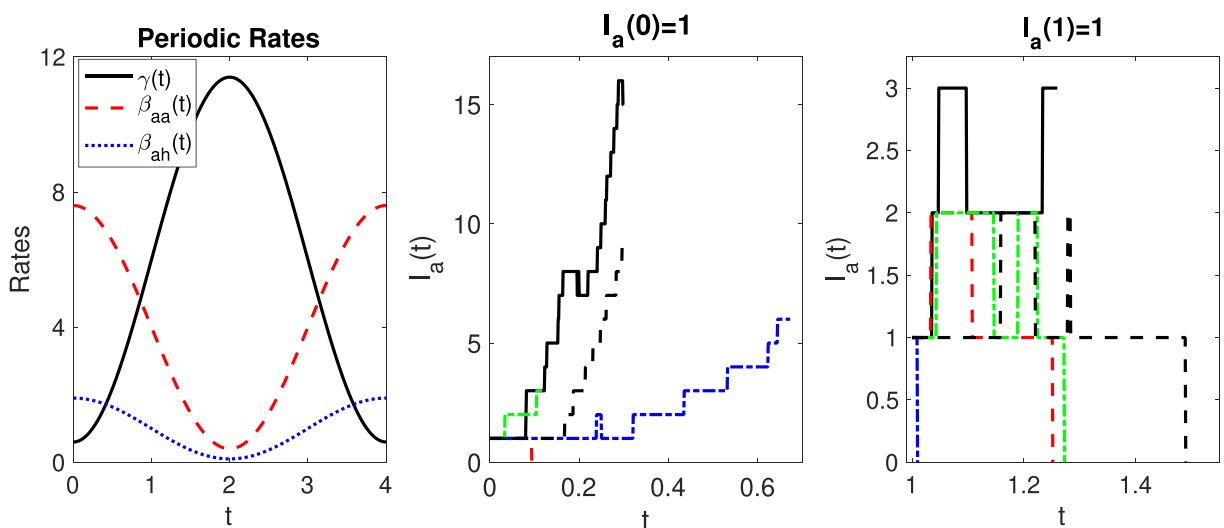


Fig. 2. Five sample paths are graphed for the infected animal population in the stochastic spillover model until either  $I_a(t) = 0$  or  $I_h(t) = 1$ ,  $t > t_0$ . Parameter values are  $N_a = 1000 = N_h$ ,  $\beta_i(t) = \beta_i(1 + 0.9\cos(\pi/2))$ ,  $i = aa, ah$ ,  $\gamma(t) = \gamma(1 - 0.9\cos(\pi/2))$ ,  $\beta_{aa} = 4$ ,  $\beta_{ah} = 1$  and  $\gamma = 6$  and initial conditions  $S_a(t_0) = 999$ ,  $I_a(t_0) = 1$ ,  $S_h(t_0) = 1000$  and  $I_h(t_0) = R_h(t_0) = R_a(t_0) = 0$  for  $t_0 = 0$  or  $t_0 = 1$ .

**Table 2**  
Transition probabilities for a branching process approximation of spillover.

Event	$(\Delta I_a, \Delta I_h)$	Probabilities
(i)	(1, 0)	$\beta_{aa}(t)i_a\Delta t + o(\Delta t)$
(ii)	(-1, 0)	$\gamma(t)i_a\Delta t + o(\Delta t)$
(iii)	(0, 1)	$\beta_{ah}(t)i_a\Delta t + o(\Delta t)$

$$G_{i,j}(u, v, t_0, t) = \sum_{k,l=0}^{\infty} p_{(i,j),(k,l)}(t_0, t) u^k v^l. \tag{6}$$

As our focus is the first human spillover, we restrict to the case  $I_h(s) = 0$  for  $s \in [t_0, t]$ , i.e.,  $j = l = 0$  in equations (5) and (6). With these restrictions, the simplified expressions for the transition probability and the generating function are defined as follows:

$$\begin{aligned} p_{i,k}(t_0, t) &\equiv p_{(i,0),(k,0)}(t_0, t), \\ G_i(u, t_0, t) &\equiv G_{i,0}(u, \mathbf{0}, t_0, t) \end{aligned}$$

in particular,

$$p_{i,k}(t_0, t) = \mathbb{P}(I_a(t) = k | I_a(t_0) = i \text{ and } I_h(s) = 0, \quad t_0 \leq s \leq t).$$

Applying the probabilities in Table 2, we derive the backward Kolmogorov differential equations for the restricted process. It follows that the transition probability for a small change in the initial time  $\Delta t_0 > 0$  equals

$$p_{i,k}(t_0 + \Delta t_0, t) = \beta_{aa}(t_0 + \Delta t_0) i p_{i+1,k}(t_0, t) \Delta t_0 + \gamma(t_0 - \Delta t_0) i p_{i-1,k}(t_0, t) \Delta t_0 + [1 - (\beta_{aa}(t_0 - \Delta t_0) + \gamma(t_0 - \Delta t_0) + \beta_{ah}(t_0 - \Delta t_0)) i] \Delta t_0 p_{i,k}(t_0, t) + o(\Delta t_0)$$

subtracting  $p_{i,k}(t_0, t)$ , dividing by  $\Delta t_0$  and letting  $\Delta t_0 \rightarrow 0^+$  yield

$$\frac{\partial p_{i,k}(t_0, t)}{\partial t_0} = \beta_{aa}(t_0) i p_{i+1,k}(t_0, t) + \gamma(t_0) i p_{i-1,k}(t_0, t) - [\beta_{aa}(t_0) + \gamma(t_0) + \beta_{ah}(t_0)] i p_{i,k}(t_0, t) \tag{7}$$

the probability of animal disease extinction at time  $t$  (with no human spillover) from one infected animal at time  $t_0$  equals

$$p_{1,0}(t_0, t) = G_1(0, t_0, t). \tag{8}$$

It follows from the branching process assumption of independence that  $G_i(u, t_0, t) = [G_1(u, t_0, t)]^i$  (Harris, 1963). This property also applies to  $p_{i,0}(t_0, t)$  when  $u = 0$ . In particular,

$$p_{i,0}(t_0, t) = [p_{1,0}(t_0, t)]^i. \tag{9}$$

using the identity (9) in the right side of equation (7) when  $i = 1$  and  $k = 0$ , setting  $p_{0,0}(t_0, t) = 1$  and simplifying yield

$$\begin{aligned} \frac{\partial p_{1,0}(t_0, t)}{\partial t_0} &= \beta_{aa}(t_0) [p_{1,0}(t_0, t)]^2 + \gamma(t_0) - [\beta_{aa}(t_0) + \gamma(t_0) + \beta_{ah}(t_0)] p_{1,0}(t_0, t), \\ &(\beta_{aa}(t_0) + \gamma(t_0) + \beta_{ah}(t_0)) [f(p_{1,0}(t_0, t), t_0) - p_{1,0}(t_0, t)], \end{aligned} \tag{10}$$

where  $f$  is defined as

$$f(u, t_0) = \frac{\beta_{aa}(t_0) u^2 + \gamma(t_0)}{\beta_{aa}(t_0) + \gamma(t_0) + \beta_{ah}(t_0)}. \tag{11}$$

the generating function  $f$  has the term  $\beta_{ah}(t_0)$  in the denominator implying animal disease extinction is conditional on no human spillover.

The partial differential equation in (10) does not depend explicitly on  $t$ . Therefore, fix  $t$  and make a change of variable  $s = t - t_0$  in equation (10) so that  $P(s) = p_{1,0}(t_0, t)$ . The following equation is solved backward in time:

$$\frac{dP(s)}{ds} = (\beta_{aa}(t-s) + \gamma(t-s) + \beta_{ah}(t-s)) [f(P(s), t-s) - P(s)], \quad P(0) = 0. \tag{12}$$

application of [Theorem B.1](#) and [Proposition B.1](#) in [Appendix B](#) show that  $P(s)$  converges monotonically and uniformly to a periodic solution  $\Phi(s)$  on  $s \in [0, T]$ . In particular,

$$P(s + kT) \rightarrow \Phi(s) \text{ as the integer } k \rightarrow \infty \text{ for } 0 \leq s \leq T. \tag{13}$$

For this branching process, the solutions of the backward and forward Kolmogorov differential equations for  $I_a(t_0) = 1$  are in agreement ([Feller, 1940](#)). After a change of variable, the asymptotic solution in (13) can be applied forward in time to  $p_{1,0}(t_0, t)$  as  $t \rightarrow \infty$ :

$$p_{1,0}(t_0, t) \rightarrow \Phi(T - t_0), \quad t_0 \in [0, T].$$

thus, given  $I_a(t_0) = 1$ , the asymptotic periodic probability for disease extinction in the animal population equals

$$\mathbb{P}_{ext}(1, t_0) = \Phi(T - t_0), \quad t_0 \in [0, T]. \tag{14}$$

It follows that the asymptotic probability of spillover for  $I_a(t_0) = 1$  equals  $1 - \mathbb{P}_{ext}(1, t_0)$ . Finally, the branching process assumption (9) leads to the expression for the asymptotic probability of spillover when  $I_a(t_0) = i$ :

$$\mathbb{P}_{spill}(i, t_0) = 1 - [\mathbb{P}_{ext}(1, t_0)]^i, \quad t_0 \in [0, T]. \tag{15}$$

To compute  $\mathbb{P}_{spill}(i, t_0)$  numerically, first we solve equation (12) for sufficiently large  $s > 0$  to obtain an accurate approximation of the periodic solution  $\Phi(s)$ . Second, we define  $\mathbb{P}_{ext}(1, t_0) = \Phi(T - t_0)$  and finally, we apply [formula \(15\)](#) which gives the desired probability of spillover.

In some special cases, the probability of spillover may have a trivial periodic solution, i.e., a constant solution. One obvious case is when the coefficients  $\beta_{aa}$ ,  $\beta_{ah}$  and  $\gamma$  are constant. Another case is when  $f(u, t_0)$  in (11) is independent of  $t_0$ ,  $f(u, t_0) \equiv f(u)$ . More generally, a trivial periodic probability of spillover occurs if there exists  $q \in (0, 1)$  such that  $f(q, t_0) = q$  for all  $t_0 \in [0, T]$ . In these cases, the probability of spillover is  $\mathbb{P}_{spill}(1, t_0) = 1 - q$ . These results are stated in the next theorem. The Proof is given in [Appendix B](#).

**Theorem 3.1.** *Assume the transmission and recovery rates are positive, continuous and periodic functions defined on  $\mathbb{R}$  with common period  $T > 0$ . In addition, assume that there exists a constant  $q \in (0, 1)$  such that  $f(q, t_0) = q$  for all  $t_0 \in [0, T]$ . Then  $q$  is the unique fixed point with this property. In addition, given  $I_a(t_0) = i$ , the asymptotic probability of spillover from the branching process approximation is constant,*

$$\mathbb{P}_{spill}(i, t_0) = 1 - q^i$$

for all  $t_0 \in [0, T]$ . In the particular case that the following ratios are constant,

$$\mathcal{R}_{aa} = \frac{\beta_{aa}(t_0)}{\gamma(t_0)} \quad \text{and} \quad \mathcal{R}_{ah} = \frac{\beta_{ah}(t_0)}{\gamma(t_0)}, \tag{16}$$

an explicit expression for  $q$  is given by

$$q = \frac{(\mathcal{R}_{aa} + \mathcal{R}_{ah} + 1) - \sqrt{(\mathcal{R}_{aa} + \mathcal{R}_{ah} + 1)^2 - 4\mathcal{R}_{aa}}}{2\mathcal{R}_{aa}}. \tag{17}$$

When the parameter values  $\beta_{aa}$ ,  $\beta_{ah}$  and  $\gamma$  are constant, the two ratios  $\mathcal{R}_{aa}$  and  $\mathcal{R}_{ah}$  can be characterized as reproduction numbers. The ratio  $\mathcal{R}_{aa}$  is the basic reproduction number for the animal population, i.e., the average number of secondary infections caused by one infected animal during the animal's infectious period ([van den Driessche & Watmough, 2002](#)). The ratio  $\mathcal{R}_{ah}$  is the spillover reproduction number, i.e., the average number of spillover infections caused by one infected animal during the animal's infectious period.

#### 4. Numerical examples

Several numerical examples are presented to illustrate how the probability of spillover depends on the three parameters,  $\beta_{aa}$ ,  $\beta_{ah}$  and  $\gamma$ . In the first example, we illustrate this dependence when the parameter values are constant and therefore, the two reproduction numbers,  $\mathcal{R}_{aa}$  and  $\mathcal{R}_{ah}$ , in [Theorem 3.1](#) are constant. In [Fig. 3](#), the probability of spillover is graphed as a function of these two reproduction numbers. An increase in either of these two reproduction numbers increases the probability of spillover. Interestingly, even if the basic reproduction number for the animal population is less than one,  $\mathcal{R}_{aa} < 1$  (no

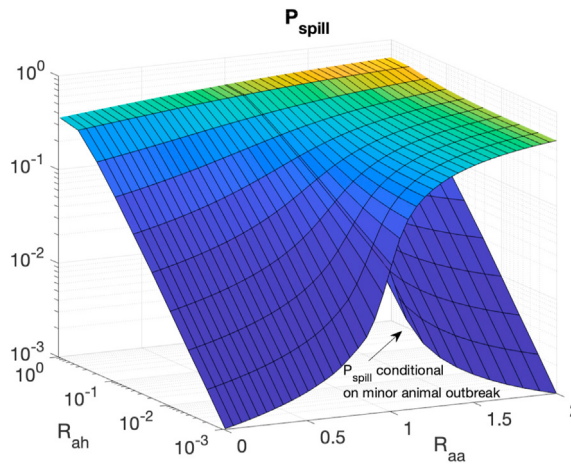


Fig. 3. The probability of spillover,  $\mathbb{P}_{spill}$ , as a function of  $\mathcal{R}_{aa}$  and  $\mathcal{R}_{ah}$  when parameter values are constant (Theorem 3.1).

major outbreaks), there may still be a spillover in the human population. But in this latter case, the spillover reproduction number  $\mathcal{R}_{ah}$  must be sufficiently large. When  $\mathcal{R}_{aa} < 1$ ,  $\mathbb{P}_{spill}$  is sensitive to the value of  $\mathcal{R}_{ah}$ . When  $\mathcal{R}_{aa} > 1$ , there are either major or minor outbreaks. For  $I_a(t_0) = 1$ , the probability of a minor animal outbreak is  $1/\mathcal{R}_{aa}$  while a major outbreak is  $1 - 1/\mathcal{R}_{aa}$  (Whittle, 1955). Hence, the probability of no spillover, conditional on a minor animal outbreak, is  $q/(1/\mathcal{R}_{aa}) = q\mathcal{R}_{aa}$  and the probability of a spillover, conditional on a minor animal outbreak, is  $1 - q\mathcal{R}_{aa}$ . Fig. 3 illustrates the difference between the probability of a spillover when there is a minor or a major outbreak. Fig. 3 agrees with Fig. 2 in Singh et al. (2014).

In the remaining numerical examples, we assume periodic transmission and recovery rates and compare the estimate of the probability of spillover in equation (15) to the value obtained from the sample paths of the time-nonhomogeneous process. For illustration purposes, suppose the transmission and recovery rates are trigonometric functions with period  $T = 4$  seasons (one season  $\approx 90$  days):

$$\beta_i(t) = \bar{\beta}_i \left( 1 + \varepsilon_i \cos\left(\frac{2\pi t}{T}\right) \right), \quad i = aa, ah, \tag{18}$$

$$\gamma(t) = \bar{\gamma} \left( 1 + \varepsilon_g \cos\left(\frac{2\pi t}{T}\right) \right), \tag{19}$$

and other parameter values are given in Table 3. The rates have units per season. The average values of the transmission and recovery rates are  $\bar{\beta}_i, i = aa, ah$  and  $\bar{\gamma}$ , respectively. The absolute values of the  $\varepsilon_i, i = aa, ah, g$  are the amplitudes of the seasonal rates.

In the numerical simulations of the Markov time-nonhomogeneous process, the events are defined as in Table 1. A total of  $10^4$  sample paths are generated for each of five different initial time points  $t_0 = 0, 1, 2, 3, 4$ , during the period  $T = 4$ . The proportions of the  $10^4$  sample paths that result in a human spillover provide numerical estimates of the probabilities of a spillover. The remaining proportions are those sample paths that result in disease extinction in the animal population with no human spillover.

In Fig. 4, it can be seen that the estimate of the spillover probabilities from the branching process solution of equation (15) are in good agreement with the numerical simulations of the time-nonhomogeneous process (blue circles) when  $I_a(t_0) = 1$  or 5. The peak values of the probabilities of spillover are close to, but shifted left of the peak values of one of the transmission rates, either  $\beta_{aa}(t_0)$  (rows (b) and (c)) or  $\beta_{ah}(t_0)$  (row (d)).

Table 3  
Parameter values for the stochastic spillover model.

Parameter	Value	Parameter	Value
$N_a$	1000 animals	$\varepsilon_i, i = aa, ah$	$\pm 0.9$
$N_h$	1000 humans	$\bar{\beta}_{aa}$	4/season
$T$	4 seasons	$\bar{\beta}_{ah}$	1/season
$\varepsilon_g$	$\pm 0.9$	$\bar{\gamma}_a$	6/season

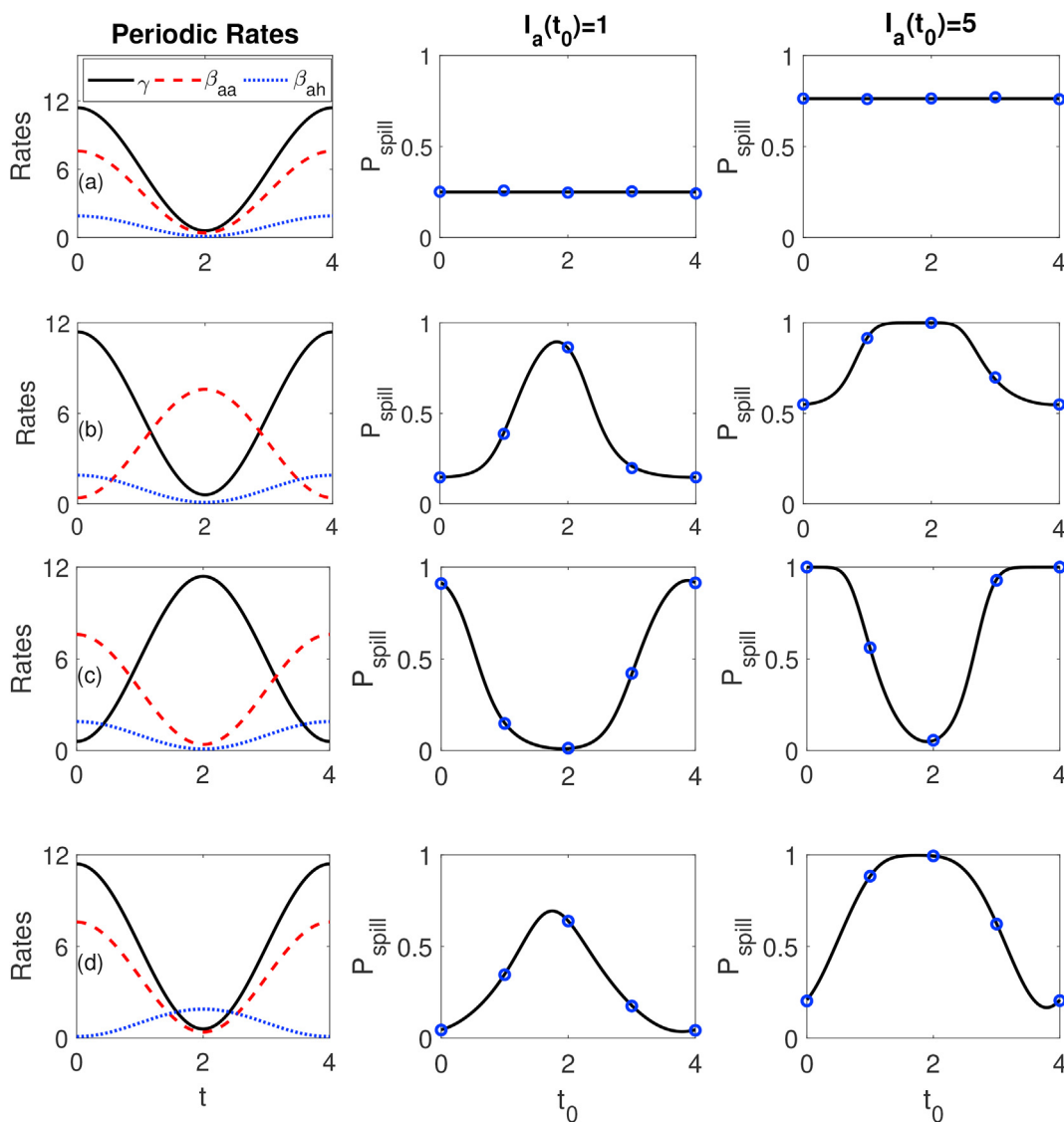


**Fig. 4.** Probabilities of spillover for different combinations of the periodic parameters  $\gamma(t)$ ,  $\beta_{aa}(t)$  and  $\beta_{ah}(t)$ . Graphs of the periodic parameters are in the left panels. The branching process estimate of probability of spillover is graphed in the middle and right panels when either one or five infected animals are introduced,  $I_a(t_0) = 1$  or 5 (black curves). Probabilities of spillover from simulation of  $10^4$  sample paths of the time-nonhomogeneous process are marked by blue circles at  $t_0 = 0, 1, 2, 3, 4$ . Parameter values are in Table 3 and periodic parameters are in equations (18)–(19). (a) First row:  $\epsilon_{aa} = \epsilon_{ah} = \epsilon_g = 0.9$ . (b) Second row:  $\epsilon_{aa} = \epsilon_{ah} = 0.9$  and  $\epsilon_g = -0.9$ . (c) Third row:  $\epsilon_{aa} = -0.9$  and  $\epsilon_{ah} = \epsilon_g = 0.9$ . (d) Fourth row:  $\epsilon_{aa} = \epsilon_{ah} = -0.9$  and  $\epsilon_g = 0.9$ .

In Fig. 5 are the graphs of the mean and standard deviation for the time until the first spillover when  $I_a(t_0) = 1$  or 5, corresponding to each of the four cases in Fig. 4. The times at which infection is initiated are  $t_0 = 0, 0.5, 1, \dots, 3.5$ . The longest mean times and greatest variability occur in case (a) when the three periodic functions have the same shape and they are all close to zero (slow change in the dynamics). The shortest mean times occur for case (c) when the transmission and the recovery rates have the reverse amplitudes, i.e., the recovery rate is fast and the transmission rates are slow.

The average probability of a spillover is computed as follows:

$$P_{spill}(i) = \frac{1}{T} \int_0^T P_{spill}(i, t_0) dt_0 \text{ for } I_a(t_0) = i. \tag{20}$$

the average probabilities for  $I_a(t_0) = 1$  or 5 are computed for each of the periodic spillover probabilities graphed in Fig. 4. They are summarized in Table 4. The results depend on the values of the periodic parameters and the initial number of animals

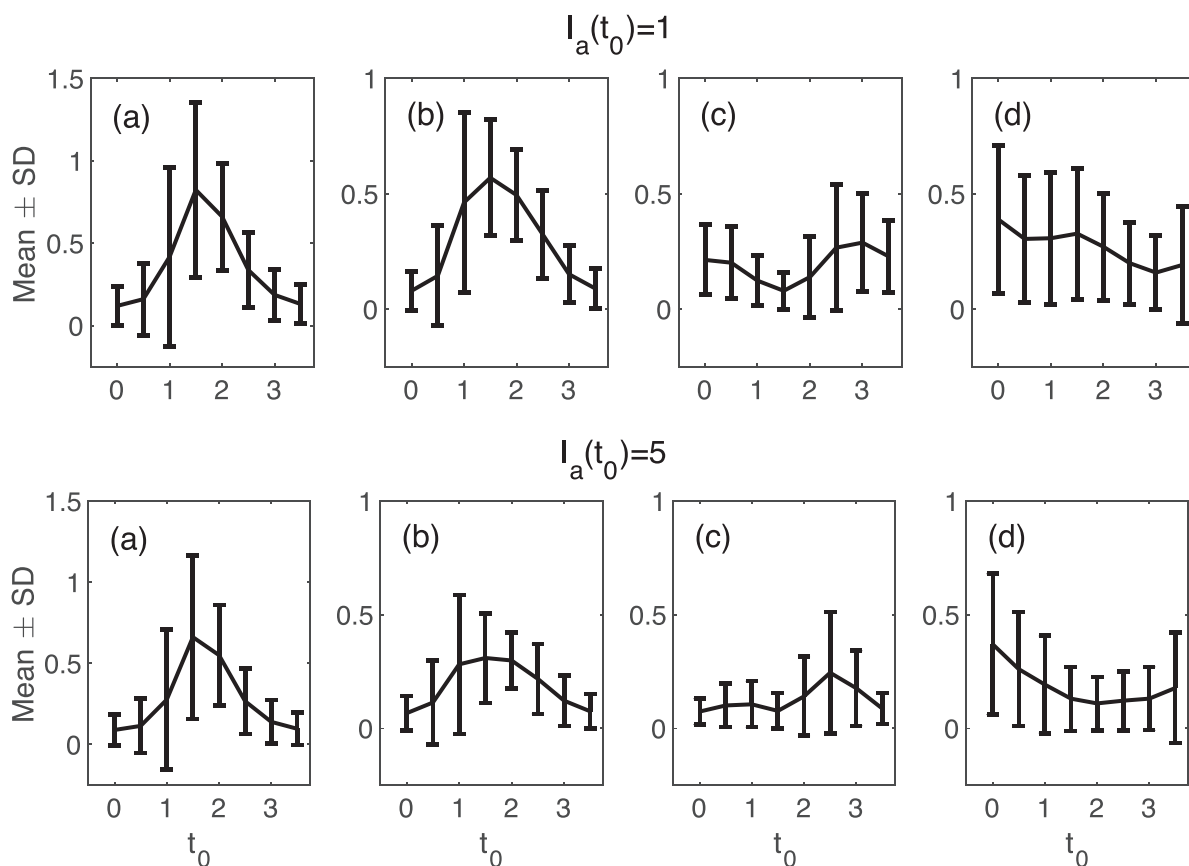


**Fig. 5.** Plots of the mean and standard deviation for the time until the first spillover event for the transmission and recovery rates given in Fig. 4 (a)–(d) when  $I_a(t_0) = 1$  or 5. The times when infected animals are introduced are  $t_0 = 0, 0.5, 1, \dots, 3.5$ .

infected. For the particular examples in Fig. 4, the average probabilities of spillover with periodic rates in (b), (c) or (d) may be greater or less than the values in case (a) which correspond to constant rates.

The role of the transmission and recovery rates in predicting the peak values of the spillover probabilities is investigated. We let the recovery rate be constant and assume the transmission rates are periodic. In Fig. 6, the probabilities of spillover are graphed for four different constant recovery rates  $\gamma = 2, 4, 6, 8$ . The transmission rates, given in equation (18), are periodic with fundamental period  $T = 4$ . In Fig. 6 (a), the transmission rates are synchronized in time with  $\beta_{aa}(t) = 4\beta_{ah}(t)$  (similar to Fig. 4 (a) and (c)). In Fig. 6 (b), the transmission rates are desynchronized in time, with  $\beta_{aa}(t)$  shifted right  $T/2$  units of  $\beta_{ah}(t)$  (similar to Fig. 4 (b) and (d)). The four graphs, top to bottom, in the right panels of Fig. 6 correspond to the four recovery rates:  $\gamma = 2, 4, 6, 8$ . As the parameter  $\gamma$  is increased, the minima and maxima of the probability of spillover switch from being dominated by the extrema of  $\beta_{aa}(t)$  to those of  $\beta_{ah}(t)$ . When  $\gamma$  increases, the average reproduction numbers decrease:  $\mathcal{R}_{aa} = \beta_{aa}/\gamma = 2, 1, 2/3, 1/2$  and  $\mathcal{R}_{ah} = \beta_{ah}/\gamma = 1/2, 1/4, 1/6, 1/8$ . In Fig. 6, if  $\mathcal{R}_{aa} \geq 1$ , the times of the peak values of the animal to animal transmission rate are more closely related to the times of highest risk of spillover than the time of the peak values of the animal to human transmission, whereas if  $\mathcal{R}_{aa} = 1/2$ , the reverse is true. For  $\mathcal{R}_{aa} = 2/3$  and  $\mathcal{R}_{ah} = 1/6$ , the spillover probability is constant,  $\mathbb{P}_{spill}(1, t_0) = 0.25$  (Theorem 3.1 and Figure B.1 in Appendix B). A similar phenomenon can be observed if  $\gamma = 6$  is fixed and the mean value of the animal to human transmission rate,  $\beta_{ah}$ , is increased from values less than one to greater than one.

### 5. Application to avian influenza

Avian Influenza (AI) is caused by influenza A viruses that are classified according to two surface proteins, hemagglutinin (H, 16 subtypes) and neuraminidase (N, 9 subtypes) (CDC, 2017). The AI viruses that infect humans are generally associated with either H5, H7 or H9 subtypes (CDC, 2019b). Outbreaks around the world of H5N1 from 2003 to July 2020, recorded by the World Health Organization, resulted in 861 confirmed human cases and 455 deaths (WHO, 2020a). An H7N9 outbreak in China from 2013 to 2015, resulted in 568 confirmed human cases and 212 deaths (WHO, 2015). A few sporadic and mild human cases have been reported for H9N2 (CDC, 2019b). Currently, none of these AI viruses have sustained human-to-human

**Table 4**  
The average probability of spillover  $P_{spill}(i)$  when the initial infected animal population is  $I_a(t_0) = 1$  or 5, based on the periodic spillover probabilities graphed in Fig. 4 (a)–(d).

Fig. 4	$P_{spill}(1)$	$P_{spill}(5)$
(a)	0.250	0.763
(b)	0.397	0.785
(c)	0.373	0.626
(d)	0.304	0.676

transmission (WHO, 2015; 2020a). The natural reservoir for AI is wild birds, specifically migrating waterfowl. Spread to humans often comes from an intermediate host, such as domestic poultry. AI viruses are also classified according to low or highly pathogenic AI (LPAI or HPAI) which refers to the severity of disease in domestic poultry (CDC, 2017). Human infection with H5N1 is often associated with HPAI while the other two, H7N9 and H9N2, are LPAI (CDC, 2017). Seasonal outbreaks of HPAI are frequently seen in domestic poultry (OIE, 2018; Tuncer & Martcheva, 2013), especially for HPAI, where seasonal migration patterns of wild birds have a strong connection with outbreaks in domestic poultry (Bui et al., 2016).

A variety of models for AI include transmission between birds and humans but only a few include seasonal variability, e.g., (Liu et al., 2017; Tuncer & Martcheva, 2013; Zhang et al., 2019). Tuncer and Martcheva (2013) applied an ODE model for spread of HPAI H5N1 between domestic poultry and humans and fit seven different models to cumulative number of human cases. The models included seasonality in domestic bird-to-bird transmission, wild bird migration, environmental transmission or a combination of all three types of seasonality. We apply the seasonal HPAI H5N1 model formulated by Tuncer and Martcheva (2013) that provided the best fit to cumulative number of human cases, the model with seasonal bird-to-bird transmission. The model also assumes replacement, removal and disease-related mortality of domestic birds but no recovery. Parameter  $\Lambda$  is the bird replacement rate,  $\mu$  is the removal rate and  $\nu$  is the disease-related mortality. In the absence of disease, the bird population is maintained at a constant population size of  $S_a = \Lambda/\mu = N_a$ . The total human population is  $N_h$ . The seasonal bird-to-bird transmission is  $\beta_{aa}(t)$ . We also consider a case with seasonal bird-to-human transmission,  $\beta_{ah}(t)$ . The ODE model (1) is replaced by the following system:

$$\text{Domestic Birds} \begin{cases} \frac{dS_a}{dt} = \Lambda - \beta_{aa}(t) \frac{I_a S_a}{N_a} - \mu S_a, \\ \frac{dI_a}{dt} = \beta_{aa}(t) \frac{I_a S_a}{N_a} - (\mu + \nu) I_a, \end{cases} \tag{21}$$

and the human population is modeled by system (2).

A Markov time-nonhomogeneous stochastic process can be defined based on the rates in the ODE models (2)–(21) as in Table 1. In this new stochastic model, there are events for replacement, removal and disease-related mortality in the domestic bird population. Approximation of the stochastic process near the DFE,  $S_a = N_a$  and  $S_h = N_h$ , leads to a branching process approximation of the time-nonhomogeneous process. Similar to the derivation of the differential equation (12), assuming  $I_a(t_0) = 1$  and defining  $s = t - t_0$ , leads to a new differential equation for the probability of no spillover for the branching process approximation of the stochastic model:

$$\frac{dP(s)}{ds} = (\beta_{aa}(t-s) + \mu + \nu + \beta_{ah}(t-s))[f(P(s), t-s) - P(s)], \quad P(0) = 0, \tag{22}$$

where the new generating function  $f$  equals:

$$f(u, t_0) = \frac{\beta_{aa}(t_0)u^2 + \mu + \nu}{\beta_{aa}(t_0) + \mu + \nu + \beta_{ah}(t_0)}. \tag{23}$$

**Table 5**  
Parameter values for domestic birds and humans. Parameter values are taken from Tuncer and Martcheva (2013) with the exception of  $N_a$ ,  $N_h$  and  $\beta_{ah}$ .

Parameter	Poultry	Parameter	Human
$N_a$	20,000 animals	$N_h$	200 humans
$\beta_{aa}$	0.1075/day	$\beta_{ah}$	0.1235/day
$\nu$	0.1/day	$T$	365 days
$\mu$	0.5/T/day		

The periodic probability of spillover for  $I_a(t_0) = 1$  is found by solving the differential equation (22) with the generating function in equation (23). To test the branching process estimate for the probability of spillover, we use the parameter values in Tuncer and Martcheva (2013), but we adjust the bird and human population sizes  $N_a$  and  $N_h$  so that they correspond to population sizes on a single large poultry farm. We also adjust  $\beta_{ah}$  so that the average reproduction numbers correspond to those in Tuncer and Martcheva (2013) (Table 5). In our model, population sizes for birds and humans are  $N_a = 20,000$  and  $N_h = 200$  and the average reproduction numbers equal

$$\bar{\mathcal{R}}_{aa} = \frac{\bar{\beta}_{aa}}{\nu + \mu} = 1.0605, \quad \bar{\mathcal{R}}_{ah} = \frac{\bar{\beta}_{ah}}{\nu + \mu} = 1.218.$$

Three different sets of periodic transmission rates for HPAI H5N1 are applied to the domestic bird-human stochastic model:

$$(i) \begin{cases} \beta_{aa}(t) = 0.1075 \left[ 1 + 0.1015 \sin\left(\frac{2\pi t}{365} + 107.75\right) \right], \\ \beta_{ah}(t) = 0.1235, \end{cases} \tag{24}$$

$$(ii) \begin{cases} \beta_{aa}(t) = 0.1075 \left[ 1 + 0.9 \sin\left(\frac{2\pi t}{365} + 107.75\right) \right], \\ \beta_{ah}(t) = 0.1235, \end{cases} \tag{25}$$

$$(iii) \begin{cases} \beta_{aa}(t) = 0.1075 \left[ 1 + 0.9 \sin\left(\frac{2\pi t}{365} + 107.75\right) \right], \\ \beta_{ah}(t) = 0.1235 \left[ 1 + 0.9 \sin\left(\frac{2\pi t}{365} + 107.75\right) \right] \end{cases} \tag{26}$$

case (i) is applied in Tuncer and Martcheva (2013). The periodic probability of spillover for these three cases are graphed in Fig. 7. There is good agreement between the branching process approximation for  $t_0 \in [0, 360]$  and the numerical simulations of the time-nonhomogeneous stochastic process for initial times  $t_0 = 0, 30, 60, 90, \dots, 360$  when  $I_a(t_0) = 1$  or  $2$  ( $10^4$  sample paths at each initial time point). The differences in amplitude and shape of the periodic transmission rates over time have a large impact on the probability of spillover. The average values of the probability of spillover are summarized in Table 6. In case (i), the average values are close to those in the model with constant transmission rates, e.g.,  $\beta_{aa}(t) = \bar{\beta}_{aa}$  and  $\beta_{ah}(t) = \bar{\beta}_{ah}$ . In cases (ii) and (iii) with more variability in the seasonality, the average values are smaller than in case (i).

### 5.1. Generalization to multiple stages

The results apply to more general spillover models that include multiple stages and seasonality. We illustrate how the spillover probabilities change with inclusion of a latent stage in the animal population. If deaths occur during the latent stage, then the probabilities of spillover will be decreased. Let the latent stage be denoted as  $E_a$ . Let the mortality rate (natural plus disease-related) be  $\mu + \alpha$  and the transition rate to the infectious stage be  $\delta$ . The ODE model for the domestic bird population is

$$\text{Domestic Birds} \begin{cases} \frac{dS_a}{dt} = \lambda - \beta_{aa}(t) \frac{I_a S_a}{N_a} - \mu S_a, \\ \frac{dE_a}{dt} = \beta_{aa}(t) \frac{I_a S_a}{N_a} - (\mu + \alpha + \delta) E_a, \\ \frac{dI_a}{dt} = \delta E_a - (\mu + \nu) I_a, \end{cases} \tag{27}$$

**Table 6**  
Average probability of spillover when the initial domestic bird population equals  $I_a(t_0) = i, i = 1, 2$  based on the branching process approximation with seasonal transmission rates as in cases (i), (ii), (iii).

Case	$\bar{P}_{spill}(1)$	$\bar{P}_{spill}(2)$
(i)	0.657	0.882
(ii)	0.651	0.875
(iii)	0.564	0.758

The rates in the domestic bird ODE model (27), coupled with the rates in the human ODE model (2), can be used to define transition probabilities for the time-nonhomogeneous stochastic model. The branching process approximation of the stochastic model at the DFE,  $S_a = \Lambda/\mu = N_a$  and  $S_h = N_h$ , and the backward Kolmogorov differential equations can be used to derive two differential equations, one for each of the variables  $E_a$  and  $I_a$  (similar to the method for derivation of (10)). A change of variable in the two differential equations,  $s = t - t_0$ , leads to the following system of differential equations:

$$\begin{aligned} \frac{dP_1(s)}{ds} &= (\delta + \mu + \alpha) [f_1(P_1(s), P_2(s), t - s) - P_1(s)] \\ \frac{dP_2(s)}{ds} &= \left( \beta_{aa}(t - s) + \mu + \nu + \beta_{ah}(t - s) \right) [f_2(P_1(s), P_2(s), t - s) - P_2(s)] \end{aligned} \tag{28}$$

with initial conditions  $P_1(0) = P_2(0) = 0$  and the two generating functions

$$\begin{aligned} f_1(u_1, u_2, t_0) &= \frac{\delta u_2 + \mu + \alpha}{\delta + \mu + \alpha}, \\ f_2(u_1, u_2, t_0) &= \frac{\beta_{aa}(t_0)u_1u_2 + \mu + \nu}{\beta_{aa}(t_0) + \mu + \nu + \beta_{ah}(t_0)}. \end{aligned}$$

The generating function  $f_1$ , given  $E_a(t_0) = 1$ , accounts for two events. Either  $E_a$  transitions to stage  $I_a$  with probability  $\delta/(\delta + \mu + \alpha)$  or dies with probability  $(\mu + \alpha)/(\delta + \mu + \alpha)$ . The generating function  $f_2$ , given  $I_a(t_0) = 1$ , also accounts for two events, conditional on no spillover. Either  $I_a$  infects another animal resulting in a new exposed animal  $E_a$  with probability  $\beta_{aa}(t_0)/(\beta_{aa}(t_0) + \mu + \nu + \beta_{ah}(t_0))$  or dies with probability  $(\mu + \nu)/(\beta_{aa}(t_0) + \mu + \nu + \beta_{ah}(t_0))$ . Numerical solution of system (28) leads to an estimate for the periodic probability of spillover:

$$P_i(s + kT) \rightarrow \Phi_i(s), \quad s \in [0, T],$$

for  $i = 1, 2$ , as  $k \rightarrow \infty$ . Thus,  $\mathbb{P}_{ext}(1, 0, t_0) = \Phi_1(T - t_0)$ ,  $\mathbb{P}_{ext}(0, 1, t_0) = \Phi_2(T - t_0)$  and

$$\mathbb{P}_{spill}(j, i, t_0) = 1 - [\mathbb{P}_{ext}(1, 0, t_0)]^j [\mathbb{P}_{ext}(0, 1, t_0)]^i, \quad t_0 \in [0, T]. \tag{29}$$

In Figure (8) are graphs of the branching process estimates of the spillover probabilities when the transmission rates are given by case (ii). Spillover is initiated by domestic birds with either one exposed bird or one infected bird:  $(E_a(t_0), I_a(t_0)) = (1, 0)$  or  $(0, 1)$ . The new parameters are  $\delta = 0.2/\text{day}$  and  $\alpha = 0.1/\text{day}$  with other parameter values in Table 5.

The average value of the periodic probability of spillover depends on the initial conditions  $(E_a(t_0), I_a(t_0)) = (j, i)$ ,  $t_0 \in [0, T]$ . It can be computed similar to formula (22) as

$$\bar{P}_{spill}(j, i) = \frac{1}{T} \int_0^T \mathbb{P}_{spill}(j, i, t_0) dt_0.$$

Table 7 is a summary of the average values for the probability of spillover for cases (i), (ii) and (iii) with either 1 or 2 exposed or infected birds.

The average values of the probabilities of spillover with an exposed stage differ from those without an exposed stage, Table 6 versus Table 7. As the exposed stage includes deaths, average values are smaller if spillover is initiated by exposed rather than by infected birds. Other generalizations of the branching process method are possible, such as spillover from indirect transmission through the environment or transmission involving several species, a natural reservoir, an intermediate host and humans.

**Table 7**

Average probability of spillover from the branching process approximation of the time-nonhomogeneous process corresponding to ODE model (2)–(27) for cases (i)–(iii) for either 1 or 2 exposed or infected birds introduced into the domestic bird population.

Case	$\bar{P}_{spill}(1, 0)$	$\bar{P}_{spill}(2, 0)$	$\bar{P}_{spill}(0, 1)$	$\bar{P}_{spill}(0, 2)$
(i)	0.414	0.656	0.624	0.858
(ii)	0.412	0.654	0.621	0.855
(iii)	0.358	0.566	0.539	0.739

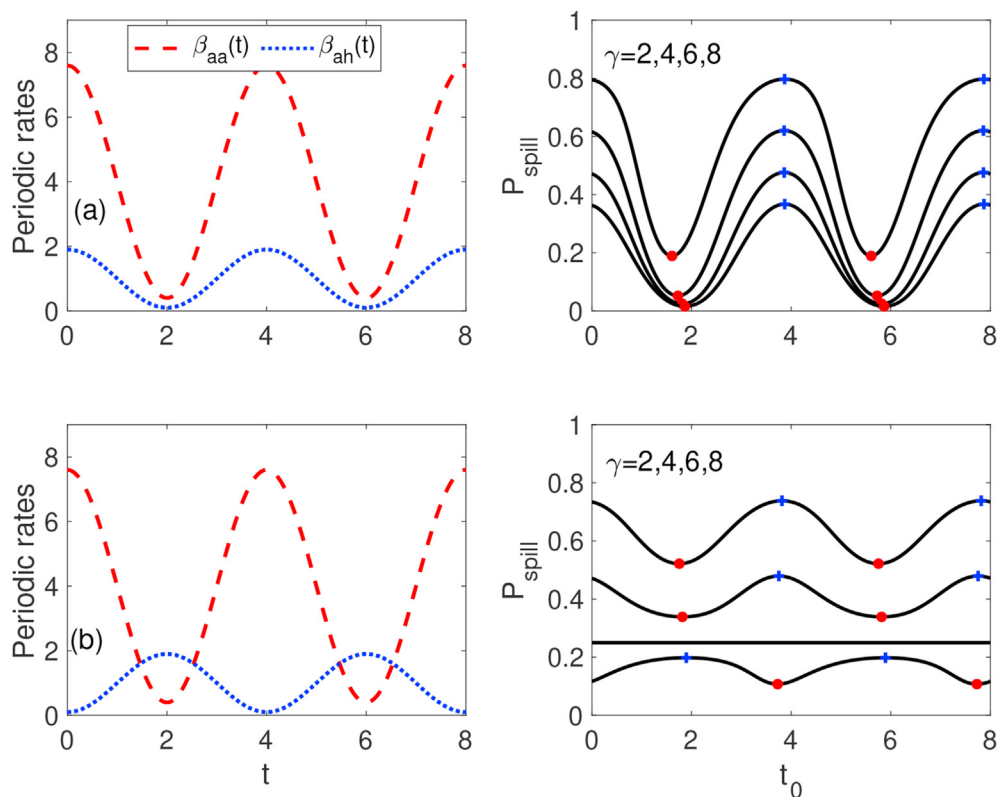


**Fig. 6.** Probability of spillover when  $\gamma$  is a fixed constant and  $\beta_{aa}(t)$  and  $\beta_{ah}(t)$  are periodic. The periodic transmission rates are graphed in the left panels and the corresponding probabilities of spillover, as computed from the branching process approximation, are graphed in right panels for four different values of  $\gamma = 2, 4, 6, 8$ . In the two panels on the right, the times at which there is greatest risk of a spillover (maximum values of  $\mathbb{P}(1, t_0)$ ) are marked with blue plus sign + and the times of lowest risk (minimum values of  $\mathbb{P}(1, t_0)$ ) are marked with a red dot •.

## 6. Discussion

Seasonality plays a crucial role in the timing of first human spillover in zoonotic diseases (Glass et al., 2000; Plowright et al., 2017; Schmidt et al., 2017). In this investigation, we generalized the mathematical results of Singh et al. (2014) by including the effects of seasonality during the early stages of an epidemic. We applied branching process theory and the backward Kolmogorov differential equations to derive an analytical approximation for the probability of the first human spillover when parameters such as the transmission and recovery rates vary seasonally. The probability of spillover depends on the time during the season when infection is introduced into the animal population. Prediction of the time of highest risk of human spillover depends on how seasonality affects the parameter rates and generally, may not be obtained by observation of a single parameter (Figs. 4 and 6).

The assumption of unbounded population sizes in the branching process limits the application of these results to large population sizes. The branching process estimates should be tested against the Markov time-nonhomogeneous process.

From a public health perspective, prevention and management of spillover require medical and veterinary approaches such as vaccination and treatment as well as ecological considerations that target transmission pathways at the human-animal interface (Karesh et al., 2012; Lloyd-Smith et al., 2009; Sokolow et al., 2019). Seasonality and changing climate are important drivers of this spillover. Understanding the role of seasonality in spillover prevention and management requires models coupled with data. Important questions for models to address are the effects of medical, veterinary and ecological interventions on public health outcomes when transmission is seasonal (Karesh et al., 2012; Lloyd-Smith et al., 2009; Schmidt et al., 2017; Sokolow et al., 2019).

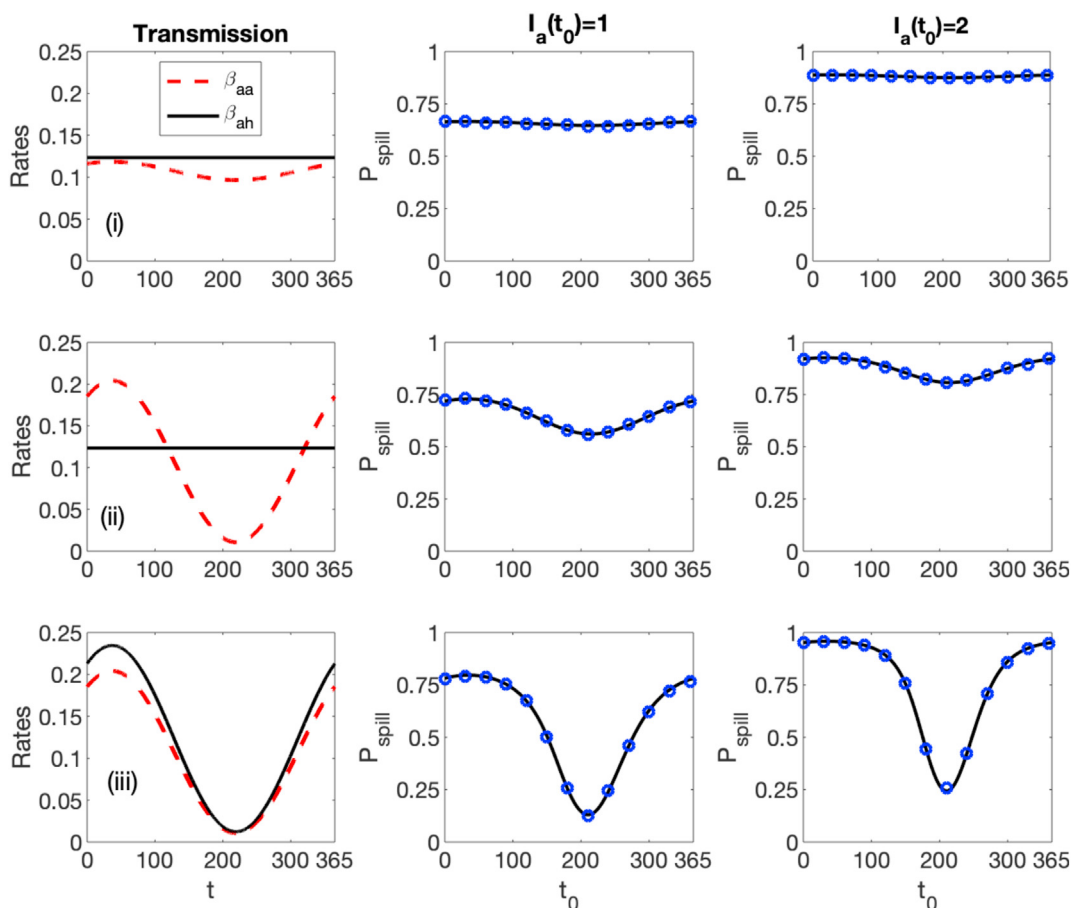


**Fig. 7.** Probability of spillover from the branching process approximation of the time-nonhomogeneous process derived from the ODE model (2)–(21). The transmission rates  $\beta_{aa}$  and  $\beta_{ah}$  are graphed in the left panels for each of the three cases (i), (ii) and (iii), equations (24)–(26), respectively. Other parameter values are given in Table 5. In the two panels on the right are the probability of human spillover, computed from the branching process approximation when either 1 or 2 infected birds are introduced into the population (black curves). From simulation of the time-nonhomogeneous process at  $t_0 = 0, 30, 60, 90, \dots, 360$ , the proportions of sample paths out of a total of  $10^4$  that result in a human spillover before death or removal of birds are also plotted (blue circles).

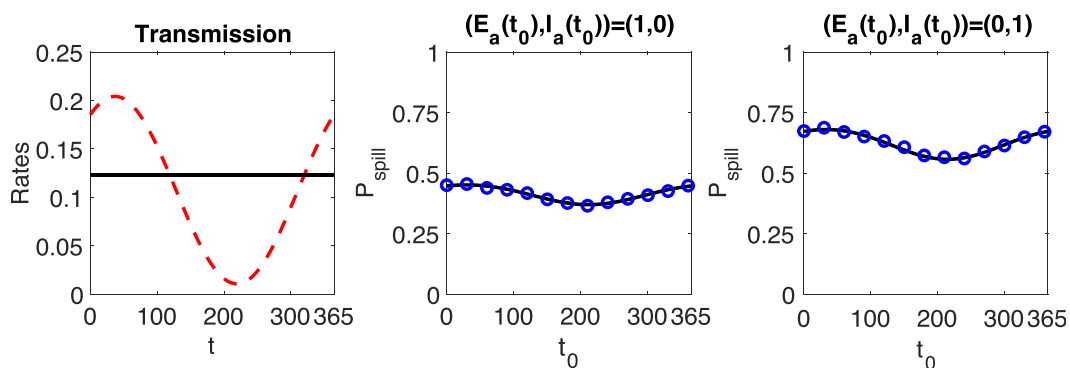


**Fig. 8.** Probability of spillover for the AI time-nonhomogeneous stochastic process corresponding to (2)–(27) with transmission rates  $\beta_{aa}$  and  $\beta_{ah}$  for case (ii). Parameters are  $\delta = 0.2/\text{day}$ ,  $\alpha = 0.1/\text{day}$  with other parameter values in Table 5. Numerical simulations from the time-nonhomogeneous process show the proportions of sample paths out of  $10^4$  that result in a human spillover before death or removal of all of the domestic birds (blue circles) at  $t_0 = 0, 30, 60, 90, \dots, 360$ .

## Declaration of competing interest

The authors declare that they have no known competing financial interests or personal relationships that could have appeared to influence the work reported in this paper.

## Acknowledgements

AN and LJS were partially supported by the National Science Foundation Grant DMS-1517719. We thank the reviewers for their helpful suggestions.

## Appendix

### A. Gillespie-type algorithm

Another method to simulate sample paths and the interevent times for the time-nonhomogeneous process is to apply a Gillespie-type algorithm. Let  $\{t_n\}_{n=0}^{\infty}$  be the times of the  $n$ th event with  $t_0$  the starting time. Let  $\Sigma(t + t_n)$  be the sum of the transition rates at time  $t + t_n < t_{n+1}$  and  $s_a, i_a$  and  $i_h$  be the values of the state variables at time  $t_n$  ( $N_h$  and  $N_a$  are constant). For the time-nonhomogeneous process defined in Table 1 and the identity (4), the value of

$$\Sigma(t + t_n) = \beta_{aa}(t + t_n)i_a \frac{S_a}{N_a} + \gamma_a(t + t_n)i_a + \beta_{ah}(t + t_n)i_a \frac{S_h}{N_h}.$$

to simulate the time until the next event (i), (ii) or (iii), the value of  $t = t_{n+1}$  is found by inverting the following function:

$$H(t) = 1 - \exp \left[ - \int_0^t \Sigma(\tau + t_n) d\tau \right]$$

that is,  $t_{n+1} = H^{-1}(1 - U) = H^{-1}(U)$ , where  $U$  is a uniform random variable on  $[0, 1]$  (Ross, 2014). This method simplifies to the well-known Gillespie algorithm when the parameters  $\beta_{aa}$ ,  $\beta_{ah}$  and  $\gamma_a$  are constant (Gillespie, 1977).

### B. Theorems

We apply the following theorems to show that  $P(s)$  converges to a periodic solution  $\Phi(s)$ ,  $s \in [0, T]$ .

**Theorem B.1.** (Theorem 4.11, p. 116 Hale and Koçak (2012)). Let  $dx/dt = h(x, t)$  with  $h(x, t + T) = h(x, t)$ , where  $h : \mathbb{R} \times \mathbb{R} \rightarrow \mathbb{R}$ . In addition, let the mapping  $(x, t) \rightarrow h(x, t)$  be a continuous function and  $C^1$  in the variable  $x$ . If a solution  $x(t)$  is bounded for  $t \geq 0$ , then there is a periodic solution  $\Phi(t)$  of period  $T$  such that

$$x(t + kT) \rightarrow \Phi(t) \text{ as the integer } k \rightarrow \pm\infty \tag{B.1}$$

monotonically and uniformly for  $0 \leq t \leq T$ .

To apply Theorem B.1 to  $P(s)$ , we show that the conditions of the theorem hold for the solution of equation (12). The function  $h$  of  $dP/ds = h(P, s)$  is a  $T$ -periodic function of  $s$  and the mapping  $(P, s) \rightarrow h(P, s)$  is a continuous function and  $C^1$  in the variable  $P$ . The following proposition also shows that  $P$  is bounded for  $s \geq 0$ .

**Proposition B.1.** Assume the transmission and recovery rates are positive, continuous and periodic functions defined on  $\mathbb{R}$  with common period  $T$ . Then the solution of the initial value problem (12) is bounded for  $s \geq 0$  and  $P(s) \notin (0, 1)$  for  $s > 0$ .

**Proof.** From the initial value problem in (12) it follows that  $dP/ds|_{s=0} > 0$ . Therefore, for small  $s$ ,  $P(s) > 0$ . If the solution of the differential equation in (12) satisfies  $P(s) \notin (0, 1)$  for some  $s > 0$ , then there exists a first time  $s_1 > 0$ , where the solution crosses the boundary of  $[0, 1]$ , either  $P(s_1) = 0$  or  $P(s_1) = 1$ . If  $P(s_1) = 0$ , from equation (12) it follows that  $dP(s)/ds|_{s=s_1} > 0$  which contradicts the fact that  $P(s)$  must be nonincreasing to cross the boundary at 0. Similarly, if  $P(s_1) = 1$ , then from equation (12),  $dP(s)/ds|_{s=s_1} < 0$  which contradicts the fact that  $P(s)$  must be nondecreasing to cross the boundary at 1. Therefore,  $P(s) \in (0, 1)$  for  $s > 0$ .

It follows from Theorem B.1 that  $P(s)$  converges monotonically and uniformly to a periodic solution  $\Phi(s)$  on  $s \in [0, T]$ . In particular,

$$P(s + kT) \rightarrow \Phi(s) \text{ as the integer } k \rightarrow \infty \text{ for } 0 \leq s \leq T.$$

The Proof of Theorem 3.1 shows in special cases that the probability of spillover is constant for all initial times  $t_0 \in [0, T]$ .

**Proof of Theorem 3.1.** Dividing the numerator and the denominator of the generating function in equation (11) by  $\gamma(t_0)$  leads to

$$f(u, t_0) = \frac{\mathcal{R}_{aa}(t_0)u^2 + 1}{\mathcal{R}_{aa}(t_0) + \mathcal{R}_{ah}(t_0) + 1}. \tag{B.2}$$

If  $f(q, t_0) = q$  for all  $t_0 \in [0, T]$ , then the identity holds for all  $t_0 \in \mathbb{R}$  as the coefficients are periodic with period  $T$ . Rewriting the differential equation for  $P$  in equation (12) in terms of the generating function in equation (B.2) yields

$$\frac{dP}{ds} = a(t-s) \left[ \frac{\mathcal{R}_{aa}(t-s)P^2 + 1}{\mathcal{R}_{aa}(t-s) + \mathcal{R}_{ah}(t-s) + 1} - P \right] = \frac{a(t-s)}{\mathcal{R}_{aa}(t-s) + \mathcal{R}_{ah}(t-s) + 1} h(P, t-s),$$

where  $u = P, t_0 = t - s,$

$$a(t-s) = \beta_{aa}(t-s) + \gamma(t-s) + \beta_{ah}(t-s)$$

and

$$h(P, t-s) = \mathcal{R}_{aa}(t-s)P^2 - (\mathcal{R}_{aa}(t-s) + \mathcal{R}_{ah}(t-s) + 1)P + 1. \tag{B.3}$$

Since  $f(q, t-s) = q$  for fixed  $t$  and all  $s \in \mathbb{R}$ , then  $h(q, t-s) = 0$  for all  $s \in \mathbb{R}$ . Rewrite the equation  $h(q, t-s) = 0$  as

$$\mathcal{R}_{aa}(t-s)q + \mathcal{R}_{ah}(t-s) \frac{q}{1-q} = 1.$$

Suppose  $0 < q_1 < q < 1$ . Then  $q_1/(1 - q_1) < q/(1 - q)$ , which implies

$$\mathcal{R}_{aa}(t-s)q_1 + \mathcal{R}_{ah}(t-s) \frac{q_1}{1-q_1} < 1$$

for all  $s \in \mathbb{R}$ . The preceding inequality implies  $h(q_1, t-s) > 0$  for all  $s \in \mathbb{R}$ . A similar argument shows for  $0 < q < q_2 < 1$  that  $h(q_2, t-s) < 0$  for all  $s \in \mathbb{R}$ . Consequently,  $q$  is the unique constant in  $(0, 1)$  with the property  $h(q, t-s) = 0$  or equivalently  $f(q, t_0) = q$ . We have shown that  $h(P, t-s) > 0$  for  $0 \leq P < q$  and  $h(P, t-s) < 0$  for  $q < P \leq 1$ . Since  $a(t-s)$  is strictly positive and bounded, it follows that  $P(s)$  converges monotonically to  $q$ . Theorem B.1 implies  $\Phi(s) = q$  and it follows that  $\mathbb{P}_{ext}(1, t_0) = \Phi(T - t_0) = q$ . In the special case that  $\mathcal{R}_{aa}$  and  $\mathcal{R}_{ah}$  are constants, equation (B.3) and application of the quadratic formula yield the explicit formula for  $q$ , expressed in equation (17).

Fig. B.1 illustrates the fixed point for the generating function  $f(P, t_0)$  corresponding to Fig. 6 (b) based on Theorem 3.1.

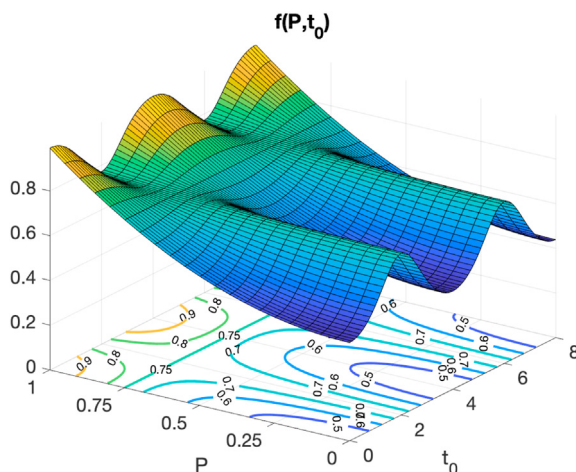


**Fig. B.1.** Graph of the generating function  $f(P, t_0)$  and the contours for the example in Fig. 6 (b) for  $\gamma = 6$ . Evident in the contours is the constant value of  $f(P, t_0)$  when  $P = 0.75$ , the fixed point of  $f$  for all time  $t_0$ .

### C. Probability density for time to spillover

In Fig. C.1 are graphed the approximate probability densities for the time to first spillover in the human population based on the transmission and recovery rates in Fig. 4 (a)–(d). Probability histograms in Fig. C.1 record the frequencies (probability  $\times 500$ ) based on  $10^4$  sample paths of the time-nonhomogeneous stochastic model that result in the first human spillover for  $I_a(t_0) = 1$  at  $t_0 = 0, 1, 2, 3$  in cases (a)–(d), respectively. The approximate means and standard deviations for these probability densities are graphed in Fig. 5 (a)–(d).

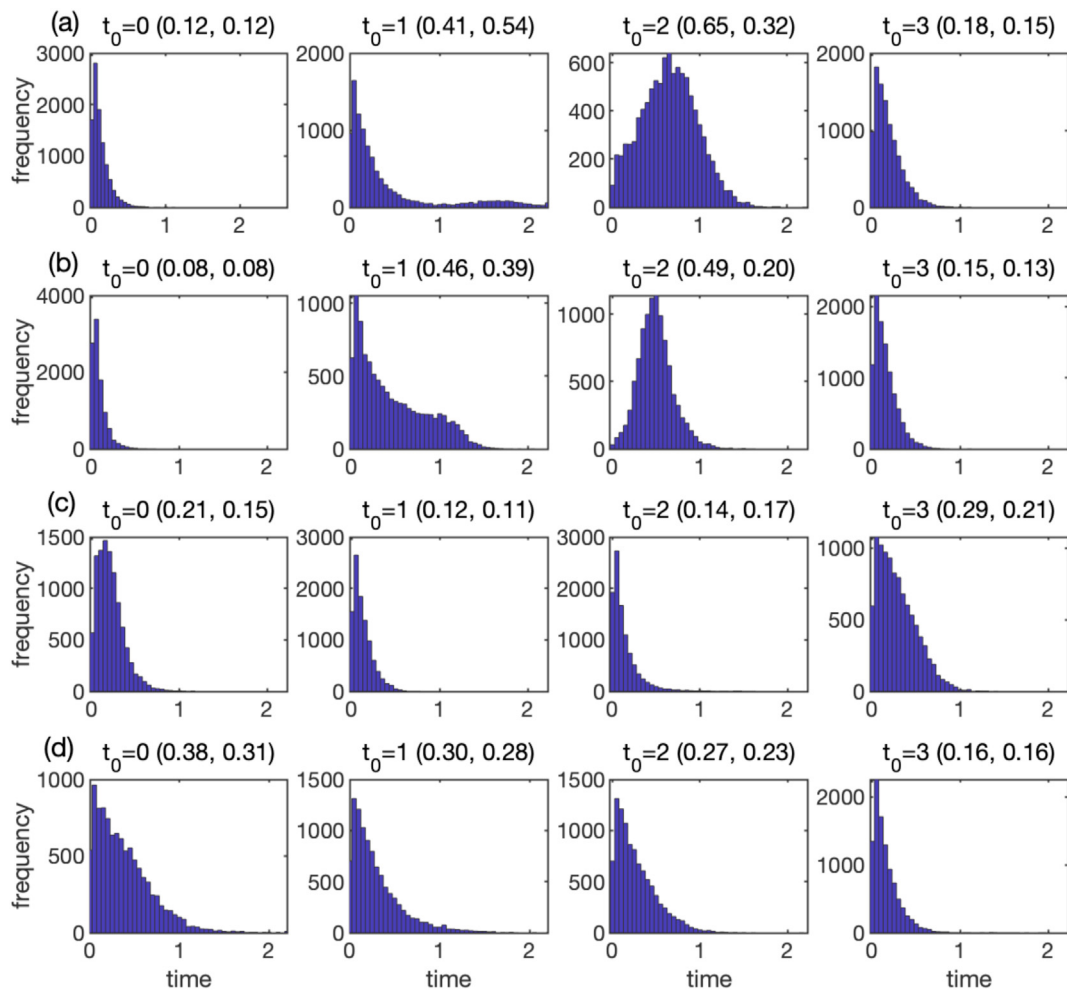


**Fig. C.1.** Probability histograms (frequency = prob  $\times 500$ ) of the time to the first human spillover, given  $I_a(t_0) = 1$  at  $t_0 = 0, 1, 2, 3$  in the time-nonhomogeneous stochastic model. Transition rates given in Table 1. Transmission and recovery rates are the same as in Fig. 4 (a)–(d). The means and standard deviations (mean, std) are recorded on the top of each panel.

### References

- Allen, L. J. S., Wesley, C. L., Owen, R. D., Goodin, D. G., Koch, D., Jonsson, C. B., ... Paige, R. L. (2009). A habitat-based model for the spread of hantavirus between reservoir and spillover species. *Journal of Theoretical Biology*, 260(4), 510–522.
- Asamoah, J. K. K., Oduro, F. T., Bonyah, E., & Seidu, B. (2017). Modelling of rabies transmission dynamics using optimal control analysis. *Journal of Applied Mathematics*, 2017. <https://doi.org/10.1155/2017/2451237>.
- Breban, R., Drake, J. M., Stallknecht, D. E., & Rohani, P. (2009). The role of environmental transmission in recurrent avian influenza epidemics. *PLoS Computational Biology*, 5(4), e1000346. <https://doi.org/10.1371/journal.pcbi.1000346>
- Bui, C., Bethmont, A., Chughtai, A. A., Gardner, L., Sarkar, S., Hassan, S., ... MacIntyre, C. R. (2016). A systematic review of the comparative epidemiology of avian and human influenza A H5N1 and H7N9—lessons and unanswered questions. *Transboundary and Emerging Diseases*, 63, 602–620.
- Calisher, C. H., Childs, J. E., Field, H. E., Holmes, K. V., & Schountz, T. (2006). Bats: Important reservoir hosts of emerging viruses. *Clinical Microbiology Reviews*, 19, 531–545.
- CDC. (2017). Centers for disease Control and prevention: Influenza type A viruses. <https://www.cdc.gov/flu/avianflu/influenza-a-vir-us-subtypes.htm>. (Accessed 4 October 2020).
- CDC. (2019a). Centers for Disease Control and Prevention. 8 zoonotic diseases shared between animals and people of most concern in the U.S. <https://www.cdc.gov/media/releases/2019/s0506-zo-onotic-diseases-shared.html>. (Accessed 15 September 2020).
- CDC. (2019b). Centers for Disease Control and Prevention. Viruses of Special Concern. <https://www.cdc.gov/flu/pandemic-resources/monitoring/viruses-concern.html>. (Accessed 17 September 2020).

- Chen, T. M., Rui, J., Wang, Q. P., Zhao, Z. Y., Cui, J. A., & Yin, L. (2020). A mathematical model for simulating the phase-based transmissibility of a novel coronavirus. *Infectious Diseases of Poverty*, 9, 1–8.
- Cui, J., Eden, J. S., Holmes, E. C., & Wang, L. F. (2013). Adaptive evolution of bat dipeptidyl peptidase 4 (dpp4): Implications for the origin and emergence of Middle East respiratory syndrome coronavirus. *Virology Journal*, 10, 304. <https://doi.org/10.1186/1743-422X-10-304>
- van den Driessche, P., & Watmough, J. (2002). Reproduction numbers and sub-threshold endemic equilibria for compartmental models of disease transmission. *Mathematical Biosciences*, 180, 29–48.
- Feller, W. (1940). On the integro-differential equations of purely discontinuous Markoff processes. *Transactions of the American Mathematical Society*, 48, 488–515.
- Gillespie, D. T. (1977). Exact stochastic simulation of coupled chemical reactions. *The Journal of Physical Chemistry*, 81, 2340–2361.
- Glass, G. E., Cheek, J. E., Patz, J. A., Shields, T. M., Doyle, T. J., Thoroughman, D. A., ... Bryan, R. (2000). Using remotely sensed data to identify areas at risk for hantavirus pulmonary syndrome. *Emerging Infectious Diseases*, 6(3), 238–247.
- Gumel, A. B. (2009). Global dynamics of a two-strain avian influenza model. *International Journal of Computer Mathematics*, 86, 85–108.
- Guo, Y. R., Cao, Q. D., Hong, Z. S., Tan, Y. Y., Chen, S. D., Jin, H. J., & Yan, Y. (2020). The origin, transmission and clinical therapies on coronavirus disease 2019 (COVID-19) outbreak—an update on the status. *Military Medical Research*, 7, 1–10. <https://doi.org/10.1186/s40779-020-00240-0>
- Hale, J. K., & Koçak, A. (2012). *Dynamics and bifurcations* (Vol. 3). Springer Science & Business Media.
- Han, H. J., Wen, H. L., Zhou, C. M., Chen, F. F., Luo, L. M., Liu, J. W., & Yu, X. J. (2015). Bats as reservoirs of severe emerging infectious diseases. *Virus Research*, 205, 1–6.
- Harris, T. E. (1963). *The theory of branching processes*. Berlin, Heidelberg: Springer-Verlag.
- Huang, J., Ruan, S., Shu, Y., & Wu, X. (2019). Modeling the transmission dynamics of rabies for dog, Chinese ferret badger and human Interactions in Zhejiang province, China. *Bulletin of Mathematical Biology*, 81, 939–962.
- Iwami, S., Takeuchi, Y., & Liu, X. (2007). Avian–human influenza epidemic model. *Mathematical Biosciences*, 207, 1–25.
- Jones, K. E., Patel, N. G., Levy, M. A., Storeygard, A., Balk, D., Gittleman, J. L., & Daszak, P. (2008). Global trends in emerging infectious diseases. *Nature*, 451, 990–993. <https://doi.org/10.1038/nature06536>
- Jonsson, C., Figueiredo, L., & Vapalahti, O. (2010). A global perspective on hantavirus ecology, epidemiology, and disease. *Clinical Microbiology Reviews*, 23, 412–441.
- Karesh, W. B., Dobson, A., Lloyd-Smith, J. O., Lubroth, J., Dixon, M. A., Bennett, M., ... Heymann, D. L. (2012). Ecology of zoonoses: Natural and unnatural histories. *The Lancet*, 380(9857), 1936–1945.
- Karlin, S., & Tavaré, S. (1982). Linear birth and death processes with killing. *Journal of Applied Probability*, 19, 477–487.
- Keeling, M. J., & Gilligan, C. A. (2000). Bubonic plague: A metapopulation model of a zoonosis. *Proceedings of the Royal Society of London. Series B: Biological Sciences*, 267, 2219–2230.
- Lau, S. K., Woo, P. C., Li, K. S., Huang, Y., Tsoi, H. W., Wong, B. H., Wong, S. S., Leung, S. Y., Chan, K. H., & Yuen, K. Y. (2005). Severe acute respiratory syndrome coronavirus-like virus in Chinese horseshoe bats. *Proceedings of the National Academy of Sciences*, 102, 14040–14045.
- Liu, S., Ruan, S., & Zhang, X. (2017). Nonlinear dynamics of avian influenza epidemic models. *Mathematical Biosciences*, 283, 118–135.
- Lloyd-Smith, J. O., George, D., Pepin, K. M., Pitzer, V. E., Pulliam, J. R., Dobson, A. P., Hudson, P. J., & Grenfell, B. T. (2009). Epidemic dynamics at the human–animal interface. *Science*, 326, 1362–1367.
- Luis, A. D., Hayman, D. T., O’Shea, T. J., Cryan, P. M., Gilbert, A. T., Pulliam, J. R. C., ... Webb, C. T. (2013). A comparison of bats and rodents as reservoirs of zoonotic viruses: Are bats special? *Proceedings of the Royal Society B: Biological Sciences*, 280. <https://doi.org/10.1098/rspb.2012.2753>
- Martinez, M. E. (2018). The calendar of epidemics: Seasonal cycles of infectious diseases. *PLoS Pathogens*, 14, Article e1007327.
- Nipa, K. F., & Allen, L. J. S. (2020). Disease emergence in multi-patch stochastic epidemic models with demographic and seasonal variability. *Bulletin of Mathematical Biology*, 82, 1–30.
- OIE. (2018). *World Organization for Animal Health: OIE situation report for highly pathogenic avian influenza*. OIE. [https://www.oie.int/fileadmin/Home/eng/Animal\\_Health\\_in\\_the\\_World/docs/pdf/OIE\\_AI\\_situation\\_report/OIE\\_SituationReport\\_AI\\_August2018.pdf](https://www.oie.int/fileadmin/Home/eng/Animal_Health_in_the_World/docs/pdf/OIE_AI_situation_report/OIE_SituationReport_AI_August2018.pdf). (Accessed 4 October 2020).
- Plowright, R. K., Parrish, C. R., McCallum, H., Hudson, P. J., Ko, A. I., Graham, A. L., & Lloyd-Smith, J. O. (2017). Pathways to zoonotic spillover. *Nature Reviews Microbiology*, 15, 502–510.
- Poen, M. J., Fouchier, R. A., Webby, R. J., Webster, R. G., & El Zowalaty, M. E. (2019). Evidence of the presence of low pathogenic avian influenza A viruses in wild waterfowl in 2018 in South Africa. *Pathogens*, 8, 163. <https://doi.org/10.3390/pathogens8040163>
- Ross, S. M. (2014). *Introduction to probability models*. Academic Press.
- Royce, K., & Fu, F. (2020). Mathematically modeling spillovers of an emerging infectious zoonosis with an intermediate host. *PLoS One*, 15, Article e0237780.
- Ruan, S. (2017). Modeling the transmission dynamics and control of rabies in China. *Mathematical Biosciences*, 286, 65–93.
- Sauvage, F., Langlais, M., & Pontier, D. (2007). Predicting the emergence of human hantavirus disease using a combination of viral dynamics and rodent demographic patterns. *Epidemiology and Infection*, 135, 46–56.
- Schmidt, J. P., Park, A. W., Kramer, A. M., Han, B. A., Alexander, L. W., & Drake, J. M. (2017). Spatiotemporal fluctuations and triggers of Ebola virus spillover. *Emerging Infectious Diseases*, 23, 415–422.
- Singh, S., Schneider, D. J., & Myers, C. R. (2014). Using multitype branching processes to quantify statistics of disease outbreaks in zoonotic epidemics. *Physical Review E*, 89. <https://link.aps.org/doi/10.1103/PhysRevE.89.032702>.
- Sokolow, S. H., Nova, N., Pepin, K. M., Peel, A. J., Pulliam, J. R. C., Manlove, K., & DeLeo, G. A. (2019). Ecological interventions to prevent and manage zoonotic pathogen spillover. *Philosophical Transactions of the Royal Society B*, 374(1782). <https://doi.org/10.1098/rstb.2018.0342>
- Taylor, L. H., Latham, S. M., & Woolhouse, M. E. J. (2001). Risk factors for human disease emergence. *Philosophical Transactions of the Royal Society of London. Series B: Biological Sciences*, 356, 983–989.
- Tuncer, N., & Martcheva, M. (2013). Modeling seasonality in avian influenza H5N1. *Journal of Biological Systems*, 21, 1340004.
- Vaidya, N. K., & Wahl, L. M. (2015). Avian influenza dynamics under periodic environmental conditions. *SIAM Journal on Applied Mathematics*, 75, 443–467.
- Vandegrift, K. J., Sokolow, S. H., Daszak, P., & Kilpatrick, A. M. (2010). Ecology of avian influenza viruses in a changing world. *Annals of the New York Academy of Sciences*, 1195, 113–128.
- Voinson, M., Alvergne, A., Billiard, S., & Smadi, C. (2018). Stochastic dynamics of an epidemic with recurrent spillovers from an endemic reservoir. *Journal of Theoretical Biology*, 457, 37–50.
- Whittle, P. (1955). The outcome of a stochastic epidemic—A note on Bailey’s paper. *Biometrika*, 42, 116–122.
- WHO. (2015). *World Health Organization. WHO risk assessment of human infections with avian influenza A (H7N9) virus*, 23 February 2015. WHO [https://www.who.int/influenza/human\\_animal\\_interface/influenza\\_h7n9/RiskAssessment\\_H7N9\\_23Feb2015.pdf?ua=1](https://www.who.int/influenza/human_animal_interface/influenza_h7n9/RiskAssessment_H7N9_23Feb2015.pdf?ua=1). (Accessed 17 September 2020).
- WHO. (2020a). *World Health Organization. Cumulative number of confirmed human cases for avian influenza A(H5N1) reported to WHO, 2003–2020*. [https://www.who.int/influenza/human\\_animal\\_interface/2020\\_10\\_07\\_tableH5N1.pdf?ua=1](https://www.who.int/influenza/human_animal_interface/2020_10_07_tableH5N1.pdf?ua=1). (Accessed 17 September 2020).
- WHO. (2020b). *World Health Organization. Neglected zoonotic diseases*. [https://www.who.int/neglected\\_diseases/diseases/zoonoses/en/](https://www.who.int/neglected_diseases/diseases/zoonoses/en/). (Accessed 17 October 2020).
- Zhang, J., Li, Y., Jin, Z., & Zhu, H. (2019). Dynamics analysis of an avian influenza A (H7N9) epidemic model with vaccination and seasonality. *Complexity ID*, 4161287, 1–15.